

Structures, Properties, and Alkali Metal Ion Transport Membrane of Polyelectrolyte Complexes Consisting of Methyl Glycol Chitosan, Glycol Chitosan, and Poly(vinyl sulfate)

YASUO KIKUCHI, NAOJI KUBOTA, and HIROSHI MITSUISHI,
Department of Environmental Chemistry and Engineering, Faculty of Engineering, Oita University, Dannoharu, Oita 870-11, Japan

Synopsis

Mixtures of methyl glycol chitosan and glycol chitosan were reacted with poly(vinyl sulfate) to form many different water-insoluble polyelectrolyte complexes (PEC) in aqueous solution at various hydrogen ion concentrations. It was revealed from elemental analyses, infrared (IR) spectroscopy, and solubilities of PEC that molecular structures of each PEC are dependent on $[H^+]$. PEC membranes were made from casting solutions of all kinds of PEC, and transport phenomena through the membrane of PEC prepared in a pH 13.0 solution were investigated under various conditions. The transport ratio of Na^+ and the electric potential difference between the left- and right-hand sides of the membrane were measured, and it is suggested that the driving force for active transport depends on the membrane potential, Donnan potential and diffusion potential. Moreover, permeability of K^+ was higher than that of Na^+ in selective transport.

INTRODUCTION

Polyelectrolyte complexes (PEC) are expected to offer many different applications because of the diversity of their structures and properties.¹⁻³ For example, PEC may be prepared in the cationic or anionic form as well as neutral polymer complexes according to the choice of components, mixing ratios, and solvent pH, and may be cast into membranes with various ion exchange capacities (0–2 mEq/g dry membrane).⁴ Consequently, when such PEC membranes with high permeability⁵ are used, it is possible to control the active and selective transport of alkali metal and halide ions, of which a great number of studies have been made recently.⁶⁻¹¹ Investigations on the PEC membrane, however, are almost limited to that of synthetic polymers, and there have been only a few papers on PEC membranes of naturally occurring polysaccharides. We have already reported that the PEC membranes of glycol chitosan-poly(vinyl sulfate),¹² methyl glycol chitosan-(carboxymethyl)dextran-poly(vinyl sulfate),¹³ and [2-(diethylamino)ethyl]dextran-(carboxymethyl)dextran-poly(vinyl sulfate)^{14,15} systems are capable of the active and selective transport of alkali metal ions.

This paper deals with chemical reactions of mixtures of methyl glycol chitosan and glycol chitosan with poly(vinyl sulfate) and general characteris-

tics of the resulting PEC. Furthermore, the active transport of Na^+ through the membrane of PEC prepared in pH 13.0 solution is discussed, focusing on the relationship between the transport ratio and the membrane potential. A description is also made on the selective transport of Na^+ and K^+ .

EXPERIMENTAL

Materials

Methyl glycol chitosan (MGC) (nitrogen content, 3.33%; intrinsic viscosity, 0.29 dL/g in 1 M NaCl solution at 25°C) and glycol chitosan (GC) (nitrogen content, 5.51%; intrinsic viscosity, 1.79 dL/g in 1 M NaCl solution at 25°C) as polycations and poly(vinyl sulfate) (PVSK) (sulfur content, 19.09%; intrinsic viscosity, 0.59 dL/g in 1 M NaCl solution at 25°C) as a polyanion were used to prepare the PEC. Sodium poly(*p*-styrenesulfonate) (NaSS) and poly(*p*-styrenesulfonic acid) (HSS) with molecular weights 1.0×10^4 and 5.0×10^5 , respectively, were adopted in the active transport experiment.

Preparation of PEC

Reactions were run in 7%, 4%, 1% HCl, pH 2.0, 6.5, 11.0, 13.0, and 5% NaOH solutions, considering that the degree of dissociation of polyelectrolytes and their conformation are influenced by the hydrogen ion concentration. The molar ratio of the reactive group of MGC to that of GC in the mixture was 1 : 1. Mixture solution (2 g/L) was added dropwise to PVSK solution (2 g/L) and vice versa, both solutions were adjusted to the same $[\text{H}^+]$, at a rate of 50 mL/30 min with stirring at 22°C. Water-insoluble PECs were thus obtained. After being left for 30 min, the precipitate was separated by centrifugation. Then, it was washed with methanol, and dried in vacuo at room temperature until no further decrease in weight occurred. Estimations of nitrogen in the PEC were carried out by the Kjeldahl method, and quantitative analyses of sulfur were performed at the Institute of Physical and Chemical Research, Japan. Infrared (IR) spectra of the PEC in a KBr pellet were taken with a Hitachi 285 spectrophotometer. The miscibilities of MGC, GC, PVSK, and PEC with a ternary solvent system (NaBr/acetone/ H_2O) were examined as described previously.¹⁶

Membrane Application

The PEC membrane was obtained from the PEC prepared in pH 13.0 solution by casting. The method of casting into a membrane and the experimental conditions were described in a previous paper.¹⁵ A diaphragm-type cell, made of poly(methyl methacrylate) and consisting of two chambers, was used in the transport experiment. After washing well with water, the PEC membrane was fixed tightly with silicone rubber between both chambers of the cell having an effective area of 4.0 cm². For the active transport, 25 mL of 0.1 M NaOH solution was placed in the right side chamber of the cell, and 25 mL of HCl (or HSS) solution of one of various concentrations including 0.1 M NaCl (or 0.1 M in repeating unit NaSS) in the left side chamber simultaneously. The cell was then put in a thermostat controlled at 30°C. At proper intervals,

0.1 mL samples from both side chambers of the cell were withdrawn and measured for the Na^+ concentration by means of an atomic absorption spectrophotometer (Shimadzu AA-640). At the same time, the concentration of Cl^- was determined by the volumetric titration with $\text{Hg}(\text{NO}_3)_2$, and the concentration of SS^- from the absorbance at 260 nm (Hitachi 100-10 spectrophotometer). The electric potential difference between the left and right sides of the membrane was obtained by measurement with a Horiba F-7 potentiometer and Ag-AgCl electrodes.

For the selective transport, 25 mL of 0.05 M NaOH and KOH solution was placed in the right side chamber of the cell, and 25 mL of HCl solution of one of various concentrations in the left side chamber. Other procedures were the same as for the active transport experiment.

RESULTS AND DISCUSSION

Polyelectrolyte Complex

Figure 1 shows the dependence of the molar ratio of the reacting groups in PVSK and $\text{MGC} + \text{GC}$ in the reaction mixture solution at the starting and end points of coagulation of the PEC upon the hydrogen ion concentration. The molar ratio, $S(\text{PVSK})/N(\text{MGC} + \text{GC})$, increased with increasing $[\text{H}^+]$, that is, larger amounts of PVSK solution were necessary to coagulate $\text{MGC} + \text{GC}$ solution as the hydrogen ion concentration was high. The reason for the above is that the degree of dissociation of MGC and GC decreases with decreasing $[\text{H}^+]$, whereas that of PVSK remains unchanged. In alkaline

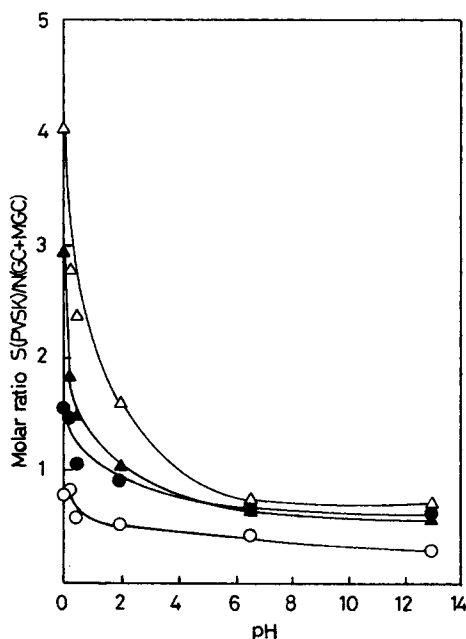


Fig. 1. Starting and end points of coagulation: (○, △) Starting points of coagulation; (●, ▲) end points of coagulation; (○, ●) PVSK solution was added dropwise to $\text{MGC} + \text{GC}$ solution; (△, ▲) $\text{MGC} + \text{GC}$ solution was added dropwise to PVSK solution.

TABLE I
Experimental Conditions, Yields, and Elemental Analyses of Polyelectrolyte Complexes

Sample code ^a	Conditions				Yield (g)	Sulfur content (%)	Nitrogen content (%)	Molar ratio of S(PVSK)/N(MGC + GC) in structural units of PEC
	Hydrogen ion concentration	S(PVSK)/N(MGC + GC) in mixture	Molar ratio of S(PVSK)/N(MGC + GC) in mixture	Molar ratio of S(PVSK)/N(MGC + GC) in structural units of PEC				
1-A	7% HCl	2.00	2.00	0.236	6.70	2.63	1.11	
1-B	4% HCl	1.60	1.60	0.252	7.02	2.98	1.03	
1-C	1% HCl	1.20	1.20	0.243	8.15	3.13	1.14	
1-D	pH 2.0	1.00	1.00	0.242	8.12	3.18	1.12	
1-E	pH 6.5	0.80	0.80	0.081	8.10	3.04	1.16	
1-F	pH 13.0	0.70	0.70	0.078	6.82	2.88	1.03	
2-A	7% HCl	2.00	2.00	0.218	6.83	2.08	1.43	
2-B	4% HCl	1.60	1.60	0.294	6.93	2.75	1.10	
2-C	1% HCl	1.20	1.20	0.363	7.68	3.10	1.08	
2-D	pH 2.0	1.00	1.00	0.464	8.17	3.22	1.11	
2-E	pH 6.5	0.50	0.50	0.567	6.51	3.19	0.89	
2-F	pH 13.0	0.50	0.50	0.440	8.19	3.13	1.14	

^aSeries 1: PVSK solution was added dropwise to MGC + GC solution (100 mL). Series 2: MGC + GC solution was added dropwise to PVSK solution (100 mL).

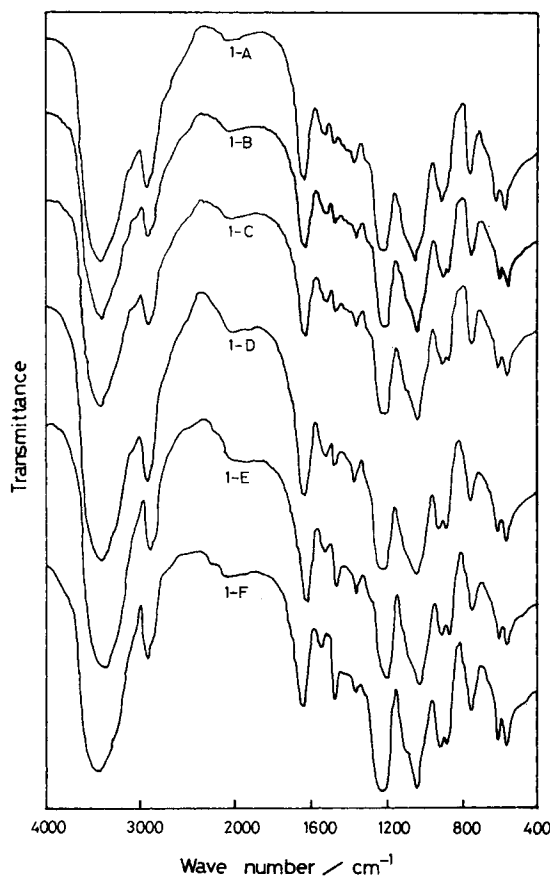


Fig. 2. IR spectra of the PEC. Sample codes correspond to those in Table I.

solution, the following strange phenomenon was observed. The coagulation occurred in pH 13.0 solution, while none in pH 11.0 solution. Further investigation of this point should be made. Experimental conditions, yields of products, and results of elemental analyses for each PEC prepared after coagulation are given in Table I. The sulfur and nitrogen contents in the PEC which reflect the molar ratio of PVS_K to MGC + GC are roughly equal. As the coagulation did not occur according to the *pK* of GC in the solution of lower $[H^+]$ than pH 6.5 in glycol chitosan-poly(vinyl sulfate) system,¹² only MGC seems to react with PVS_K in the solution of $[H^+] < \text{pH } 6.5$. Thus, the hydrogen ion concentration in this system plays an important role in determining the ratio of PVS_K/(MGC + GC) in the PEC.

Since IR spectra of the PEC prepared in the cases where PVS_K solution was added to MGC + GC solution are identical with those for the cases where MGC + GC solution was added to PVS_K solution, only the former are shown in Figure 2. IR spectra of the PEC are almost the same as that of a mixture of MGC, GC, and PVS_K, differing from one another only in detail. The absorption band at 1540 cm^{-1} assigned to $-\text{NH}_3^+$ in GC is present in all PEC except for the PEC prepared in pH 13.0 solution, and that assigned to $-\text{NH}_2$ which should appear at 1590 cm^{-1} is absent. The absorption bands at 1230 and

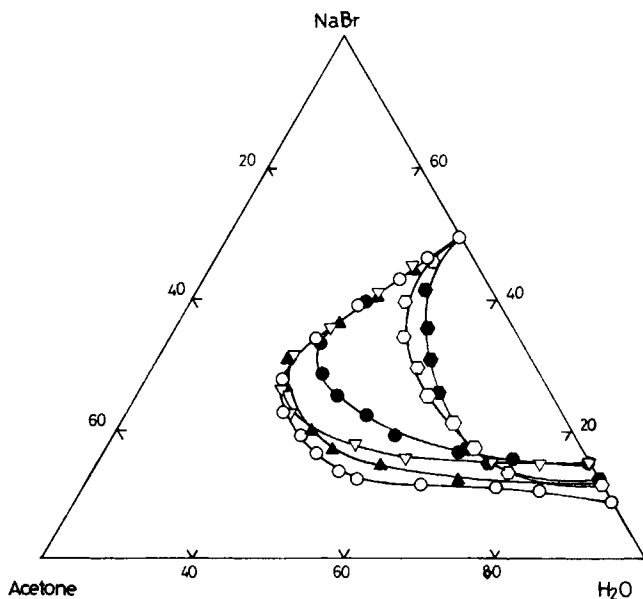


Fig. 3. Phase diagrams of PEC in the ternary solvent system at 30°C: (○) 7% HCl; (▲) 4% HCl; (▽) 1% HCl; (●) pH 2.0; (○) pH 6.5; (●) pH 13.0.

800–600 cm^{-1} , which are also present in each PEC, are assigned to $-\text{OSO}_3^-$ in PVSK. The intensity of these absorptions is nearly equal in all PEC. Furthermore, the absorption bands around 3500 cm^{-1} assigned to $-\text{OH}$ groups are found in every PEC, and this proves that the inter- and intramolecular hydrogen bonds between $-\text{OH}$ groups are formed. These results imply that the PEC were produced in the same way except for in pH 13.0 solution, when PEC was prepared after coagulation.

PEC are insoluble in common organic solvents (e.g., *N,N*-dimethylformamide, *N,N*-dimethylacetamide, and dimethyl sulfoxide), but soluble in the specific ternary solvent mixtures (e.g., NaBr/acetone/ H_2O and $\text{CaCl}_2/1,4$ -dioxane/ H_2O), and also in 36% HCl solution without heating. The phase diagrams were obtained for all kinds of PEC in the system of NaBr/acetone/ H_2O and are indicated in Figure 3. There is a small region in the solvent composition field where the PEC remains in the solution to form a homogeneous, viscous syrup. The miscibility limit of the PEC prepared in acidic solution is different from that of the PEC prepared in alkaline solution.

These experimental results support the concept that the PEC prepared in acidic solutions have common constituents and similar compositions, but the PEC prepared in alkaline solutions are different from them. This concept is attributed to the degree of dissociation of MGC, GC, and PVSK which changes according to $[\text{H}^+]$.

Polyelectrolyte Complex Membrane

The membrane obtained by casting the PEC prepared in pH 13.0 solution was adopted for the study on the transport of alkali metal ions, because this membrane was stable in acidic and alkaline solutions as shown in Table II. The concentrations of Na^+ in the left- and right-hand side chambers of the

TABLE II
Stabilities of Polyelectrolyte Complex Membranes^a in Acidic and Alkaline Solution
for 1 Day Duration

Sample code ^b	pH 1	pH 13	Sample code ^b	pH 1	pH 13
1-A	○	△	2-A	○	○
1-B	○	△	2-B	○	△
1-C	○	△	2-C	○	△
1-D	△	△	2-D	○	△
1-E	×	×	2-E	×	×
1-F	○	△	2-F	○	○

^aCast condition: 30°C, 50% relative humidity.

^bSample codes correspond to those in Table I.

Key: (○) Very stable; (△) stable; (×) soluble.

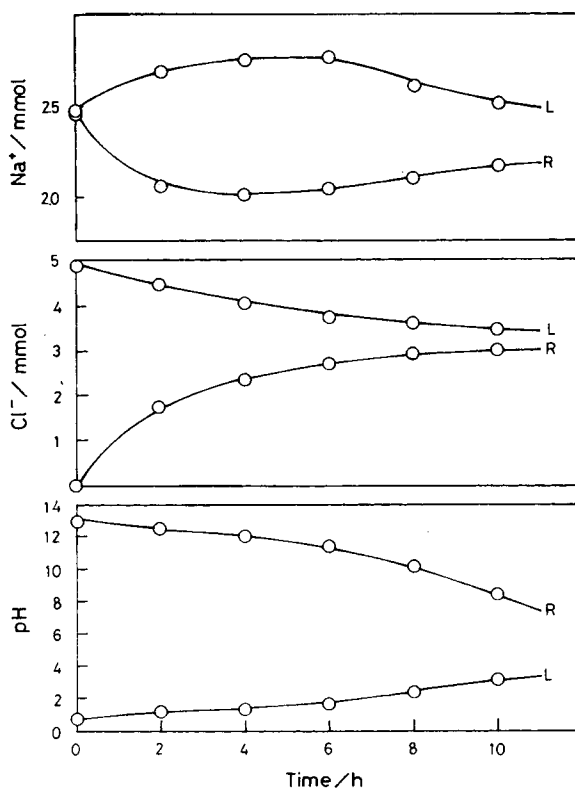


Fig. 4. Changes in concentrations of Na^+ , Cl^- , and H^+ at active transport.

cell were set the same initially. The left side chamber contained HCl as well, while the right side chamber NaOH. Figure 4 shows the concentration changes in Na^+ , Cl^- , and H^+ with the passage of time in both side chambers, when the left chamber is containing 0.1 M HCl. Despite the fact that both sides of the membrane were originally equal in the concentration of Na^+ , an increase of Na^+ in the left side was observed and the change in the right side was the reverse. This suggests that active transport of Na^+ took place from the right side, alkaline solution, to the left side, acidic solution, through the membrane. The concentration of Na^+ in the left side increased up to a maximum, and

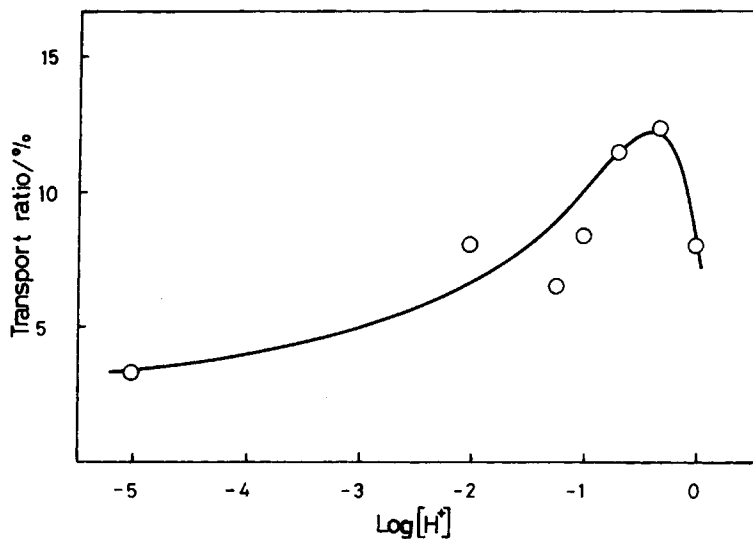


Fig. 5. Effect of the hydrogen ion concentration on the transport ratio of Na^+ in the case where HCl was used.

then decreased with time. This back transport of the concentrated Na^+ is due to the decrease in the hydrogen ion concentration difference between both sides of the membrane and to the permeation of Cl^- . The ratios of the transported ions were calculated from the following equation:

$$\text{Transport ratio (\%)} = \frac{[\text{Na}^+]_{\text{max}} - [\text{Na}^+]_0}{[\text{Na}^+]_0} \times 100 \quad (1)$$

where $[\text{Na}^+]_{\text{max}}$ is the mole number of Na^+ in the left side chamber at the maximum, and $[\text{Na}^+]_0$ is the mean of the initial mole numbers of Na^+ in both side chambers. The dependence of the transport ratio of Na^+ on the concentration of H^+ in the left side chamber is shown in Figure 5. The transport ratio corresponds to $[\text{H}^+]$, and it is thought that the driving force for the transport of Na^+ is the hydrogen ion concentration difference between both side chambers which causes the electric potential gradient. Accordingly, the membrane potential difference needs to be measured. Figure 6 indicates that the membrane potential difference is greater as the concentration of HCl in the left side is increased, and this effect is consistent with the result in Figure 5. The membrane potential difference, however, decreases with time. This decrease in the potential difference is due not only to the transport of Na^+ from the right to left side, but also to the permeation of Cl^- from the left to right side. As shown in Figure 4, this Cl^- permeation is large, therefore, an investigation of the transport for the cases where all negative charges are fixed in the left side of the membrane was attempted, and results obtained were compared with the above conclusion.

The results for the case where HSS and NaSS were adopted instead of HCl and NaCl, respectively, are displayed in Figures 7 and 8. The transport ratios were evaluated by Eq. (1) considering the transfer of water based on Donnan osmosis. The concentration of Na^+ in the left side chamber increased and that in the right side decreased with time in a similar manner as in the case of HCl.

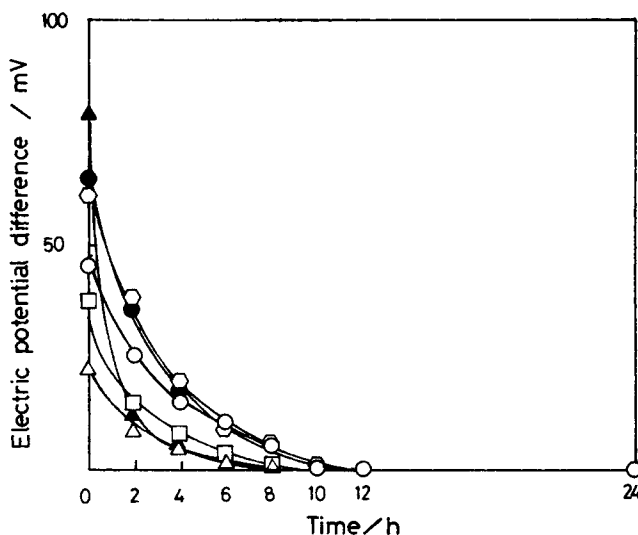


Fig. 6. Changes in the electric potential difference with time: (\blacktriangle) 1 M HCl; (\bullet) 0.5 M HCl; (\circ) 0.2 M HCl; (\circ) 0.1 M HCl; (\square) 0.05 M HCl; (\triangle) 0.01 M HCl.

On the other hand, the concentration of SS^- was unchanged, in contrast with Cl^- in the case of HCl. Moreover, the transport ratios of Na^+ were rather larger than those in the case of HCl, as shown in Figure 8. This seems to be because the membrane potential difference was maintained for a long time since SS^- is fixed thoroughly on the left side of the membrane. This assumption is supported by the result in Figure 9. The membrane potential difference was maintained even 24 h later.

Therefore, on the basis of the results mentioned above we speculate that the transport of Na^+ is achieved in the following manner. The PEC membrane is considered to be a sort of charged membrane for which the functional groups of $-OSO_3^-$ in PVSK are responsible. The transport phenomena in the case where a charged membrane is used or a certain ion is fixed in one side of the membrane is explained in terms of the Donnan membrane equilibrium. It is difficult to analyze a system such as used in this study comprising many kinds of ions. However, on the assumption that the membrane potential is the concentration membrane potential raised by HCl or HSS, the membrane potential $\Delta\phi$ can be regarded as the sum of the Donnan potentials $\Delta\phi_{Don, L}$ and $\Delta\phi_{Don, R}$ at the two solution-membrane interfaces and the diffusion potential $\Delta\phi_{Dif}$ in the membrane.¹⁷ This is represented, for example, by the following equation:

$$\begin{aligned} \Delta\phi &= \Delta\phi_{Don, L} + \Delta\phi_{Dif} + \Delta\phi_{Don, R} = \Delta\phi_{Don} + \Delta\phi_{Dif} \\ &= -\frac{RT}{F} \ln \frac{\xi_R \sqrt{1 + (2\xi_L)^2} + 1}{\xi_L \sqrt{1 + (2\xi_R)^2} + 1} - \frac{RT}{F} W \ln \frac{\sqrt{1 + (2\xi_R)^2} + W}{\sqrt{1 + (2\xi_L)^2} + W} \quad (2) \\ \xi_L &= \sqrt{\frac{k_+ k_-}{\gamma_+ \gamma_-} \frac{C_L}{X}}, \quad \xi_R = \sqrt{\frac{k_+ k_-}{\gamma_+ \gamma_-} \frac{C_R}{X}}, \quad W = \frac{\omega_+ - \omega_-}{\omega_+ + \omega_-} \end{aligned}$$

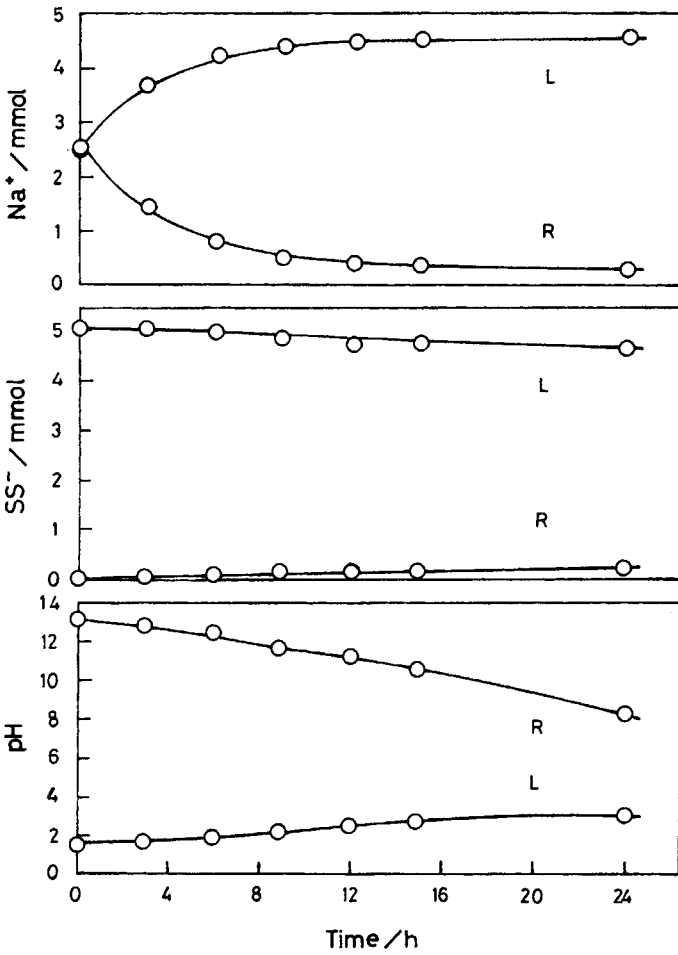


Fig. 7. Changes in concentrations of Na^+ , SS^- , and H^+ at active transport.

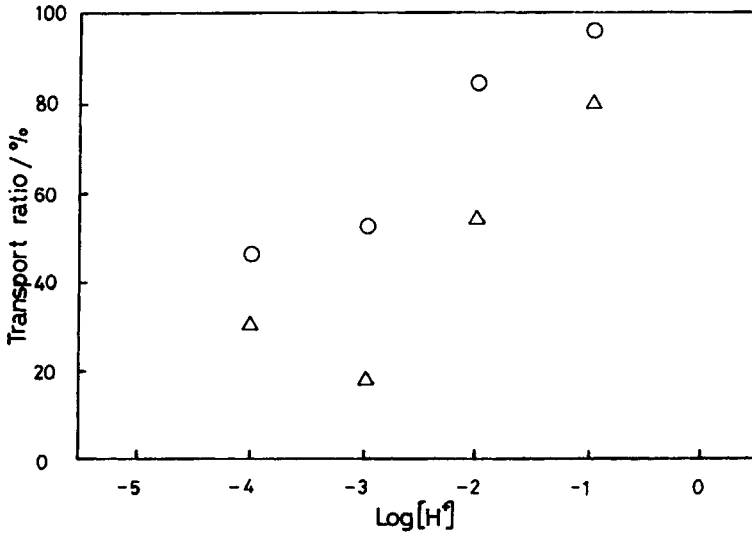


Fig. 8. Effect of the hydrogen ion concentration on the transport ratio of Na^+ in the case where HSS was used: (Δ) $M = 1.0 \times 10^4$; (\circ) $M = 5.0 \times 10^5$.

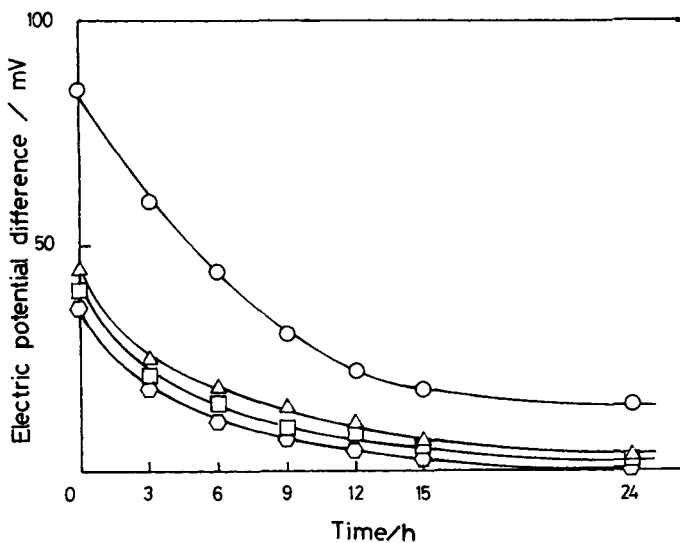


Fig. 9. Changes in the electric potential difference with time: (○) 0.1 M in repeating unit HSS ($M = 1.0 \times 10^4$); (△) 0.01 M in repeating unit HSS ($M = 1.0 \times 10^4$); (◻) 0.001 M in repeating unit HSS ($M = 1.0 \times 10^4$); (○) 0.0001 M in repeating unit HSS ($M = 1.0 \times 10^4$).

where C_L and C_R are the concentrations of electrolytes on the left side and the right side of the membrane, respectively, X is the concentration of the fixed charge in the membrane, and k_+ , k_- , γ_+ , γ_- , and ω_+ , ω_- are the distribution coefficient, the activity coefficient, and the mole mobility of cations and anions, respectively. When C_L is larger than C_R , $\Delta\phi_{Don}$ and $\Delta\phi_{Dif}$ are positive and $\Delta\phi$ is also positive as a result. A tentative membrane potential and transfer of Na^+ deduced from the conclusions described are illustrated in Figure 10. In this system, the membrane surface potential is low because PEC

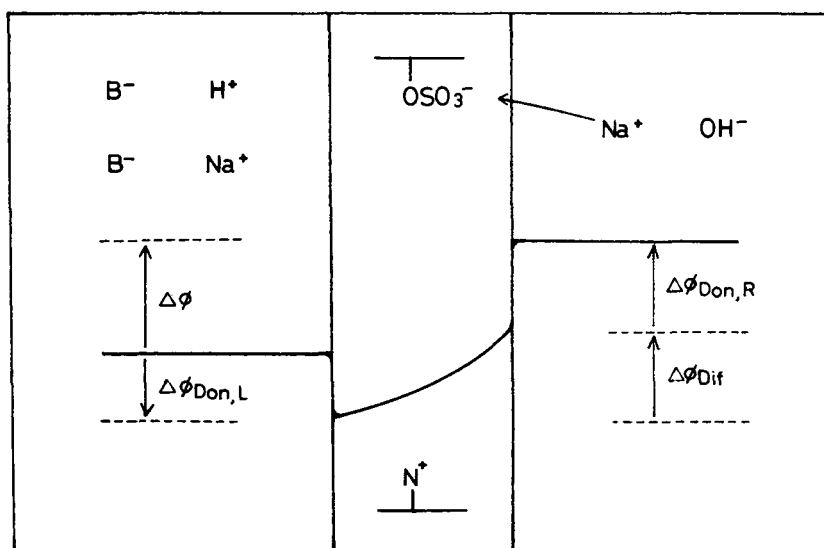


Fig. 10. Schematic representation of the membrane potential.

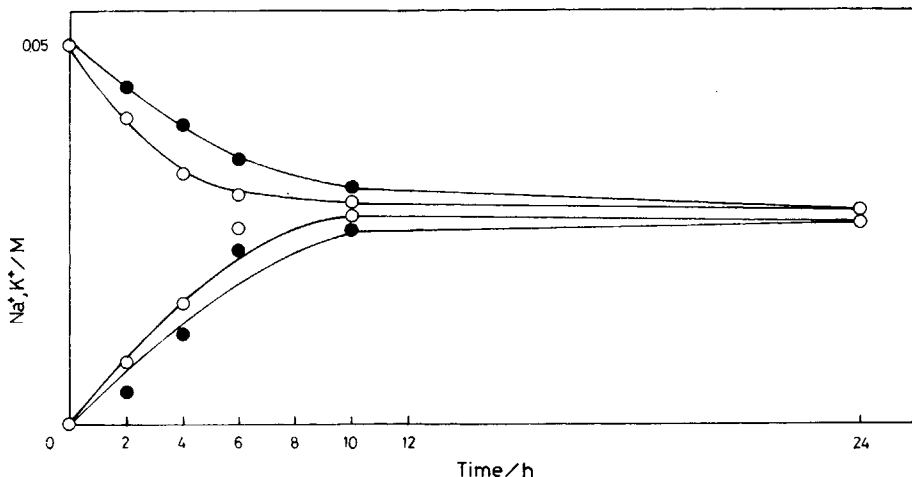


Fig. 11. Changes in concentrations of Na^+ and K^+ at selective transport: (●) Na^+ ; (○) K^+ .

membrane is anionic owing to the ratio of S(PVSK)/N(MGC + GC) (Table I), and the potential in the membrane increases in the direction toward the right because of the large mobility of H^+ . Thus, the right side is higher than the left side in the electric potential. As a result, Na^+ was transported from the right to left side, that is, from the alkaline to acidic side, through the membrane in accord with the gradient of the electric potential. It is probable that $-\text{OSO}_3^-$ groups in the membrane serve as carriers for Na^+ . However, there are $-\text{N}^+$ groups in the membrane capable of attracting Cl^- and the Donnan exclusion for Cl^- was small, so that the membrane potential difference is not maintained so long due to Cl^- permeation. Then, it seems that the transport ratio of Na^+ was low in the case of HCl. In the case of HSS, on the contrary, $\Delta\phi_{\text{Don}, L}$ and $\Delta\phi_{\text{Dif}}$ are larger than those in the case of HCl for the fixed SS^- , although $\Delta\phi_{\text{Don}, R}$ is equal. Therefore, the retention time of the membrane potential difference is long, and the transport of Na^+ in accord with the membrane potential gradient is appreciable.

The selective transport of alkali metal ions through the membrane was observed under 0.05 M NaOH and KOH solution in the right side chamber. Figure 11 shows the concentration changes in alkali metal ions in both side chambers with the passage of time, when the left side chamber was containing 0.1 M HCl solution. It is found that K^+ permeated faster than Na^+ , and it is thought that this permeability depends on the affinity of the carrier in the membrane for alkali metal ions or the diameter of those hydrated ions.⁹ Then, the ratios of transported ions were calculated by

$$\text{Selectivity} = \frac{[\text{K}^+]/[\text{K}^+]_0}{[\text{Na}^+]/[\text{Na}^+]_0} \quad (3)$$

where $[\text{K}^+]$ and $[\text{Na}^+]$ are the concentrations of K^+ and Na^+ in the left side chamber, respectively, and $[\text{K}^+]_0$ and $[\text{Na}^+]_0$ are the initial concentrations of K^+ and Na^+ in the right side chamber, respectively. The selectivity of the alkali metal ion transport through the membrane after 2 h at different

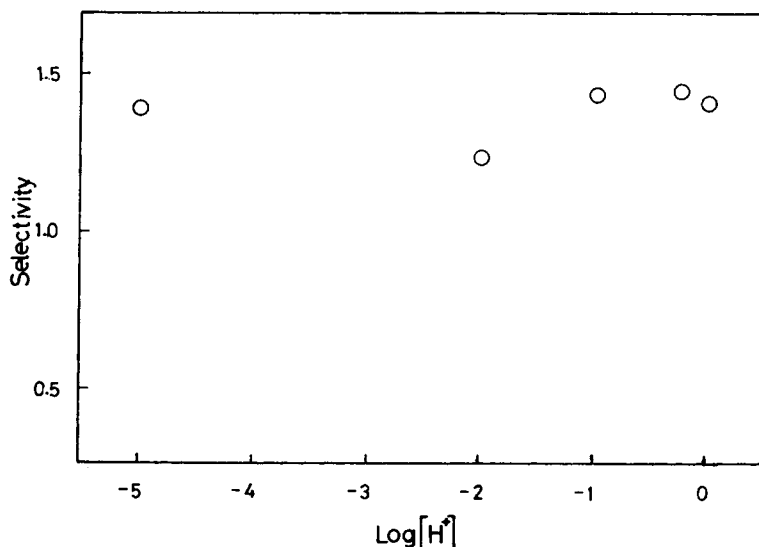


Fig. 12. Effect of the hydrogen ion concentration on the selectivity in the Na⁺ and K⁺ transport after 2 h.

hydrogen ion concentrations on the right side of the membrane is shown in Figure 12. The ratios of the transported K⁺ to Na⁺ are larger than 1.0, and nearly equal over the hydrogen ion concentration range 10⁻³ to 10⁰ M. PEC membrane in this system is regarded as a hydrogel membrane, and alkali metal ions appear to diffuse in this membrane. Therefore, it seems that the selectivity is not dependent upon [H⁺] in the left side of the membrane, and the functional group in the membrane little affects the selective transport of alkali metal ions.

References

1. Y. Mori and H. Tanzawa, *Kobunshi*, **22**, 616 (1973).
2. A. Nakajima, *Kagaku To Kogyo*, **27**, 750 (1974).
3. E. Tsuchida and K. Abe, *Adv. Polym. Sci.*, **45**, 18 (1982).
4. L. L. Markley, H. J. Bixler, and R. A. Cross, *J. Biomed. Mater. Res.*, **2**, 145 (1968).
5. H. J. Bixler and A. S. Michaels, *Encycl. Polymer Sci. Technol.*, **10**, 765 (1969).
6. T. Shimidzu, M. Yoshikawa, M. Hasegawa, and K. Kawakatsu, *Macromolecules*, **14**, 170 (1981).
7. T. Shimidzu and M. Yoshikawa, *Nippon Kagaku Kaishi*, **1983**, 958.
8. T. Uragami, R. Nakamura, and M. Sugihara, *Polymer*, **24**, 559 (1983).
9. T. Uragami, F. Yoshida, and M. Sugihara, *J. Appl. Polym. Sci.*, **28**, 1361 (1983).
10. N. Ogata, K. Sanui, and H. Fujimura, *J. Appl. Polym. Sci.*, **25**, 1914 (1980).
11. M. Yoshikawa, H. Ogata, and K. Sanui, *Polym. J.*, **15**, 609 (1983).
12. Y. Kikuchi and N. Kubota, *Bull Chem. Soc. Jpn.*, **60**, 375 (1987).
13. Y. Kikuchi and N. Kubota, *Nippon Kagaku Kaishi*, **1985**, 1592.
14. Y. Kikuchi and N. Kubota, *Nippon Kagaku Kaishi*, **1985**, 111.
15. Y. Kikuchi and N. Kubota, *J. Appl. Polym. Sci.*, **30**, 2565 (1985).
16. Y. Kikuchi, K. Hori, and Y. Onishi, *Nippon Kagaku Kaishi*, **1980**, 1157.
17. T. Hanai, *Maku To Ion*, Kagaku Dojin, Kyoto, 1978, p. 232.

Received October 29, 1986

Accepted April 30, 1987